

Counterstreaming electrons in magnetic clouds

S. Shodhan,¹ N. U. Crooker,¹ S. W. Kahler,² R. J. Fitzenreiter,³ D. E. Larson,⁴
R. P. Lepping,³ G. L. Siscoe,¹ and J. T. Gosling⁵

Abstract. Two widely used signatures of interplanetary coronal mass ejections are counterstreaming suprathermal electrons, implying magnetic structures connected to the Sun at both ends, and magnetic clouds, characterized by large-scale field rotations, low temperature, and high field strength. In order to determine to what extent these signatures coincide, electron heat flux data were examined for 14 magnetic clouds detected by ISEE 3 and IMP 8 near solar maximum and 34 clouds detected by Wind near solar minimum. The percentage of time during each cloud passage that counterstreaming electrons were detected varied widely, from 6 clouds with essentially no counterstreaming to 8 clouds with nearly 100% counterstreaming. All of the former but less than half of the latter occurred near solar minimum, suggesting a possible solar cycle dependence on the degree of magnetic openness. The counterstreaming intervals were distributed randomly throughout the clouds, with a median length of 2.5 hours. A plot of counterstreaming percentages against cloud diameter for 33 clouds modeled as cylindrical flux ropes indicates a linear dependence of the percentage of closed flux on cloud size, with the largest clouds being the most closed. Overall the results are consistent with the view that although magnetic field lines within a magnetic cloud can form a large-scale, coherent structure, reconnection in remote regions of the structure, presumably near the Sun, sporadically alters its topology from closed to open until the cloud assimilates into the ambient solar wind.

1. Introduction

Of the many signatures used to identify coronal mass ejections (CMEs) in the solar wind [e.g., *Zwickl et al.*, 1983; *Gosling*, 1990; *Neugebauer and Goldstein*, 1997], two widely and independently used indicators of CME passage are counterstreaming suprathermal electrons [e.g., *Gosling et al.*, 1987a] and magnetic clouds [e.g., *Burlaga*, 1991]. Counterstreaming (or bidirectional) suprathermal electrons were first identified with interplanetary ejecta from the Sun by *Montgomery et al.* [1974]. Since suprathermal electrons carry electron heat flux away from the Sun along magnetic field lines, when found streaming in both directions along the field, they are interpreted as signatures of closed magnetic field lines, most likely with both ends connected to the Sun. Intervals of counterstreaming electrons in ISEE 3 data ranging in length from 2 hours to a few days at first were treated as independent events and were successfully used for a number of studies to define other properties of ejecta such as flow deviations [*Gosling et al.*, 1987b] and geoeffectiveness [*Gosling et al.*, 1990, 1991]. Later studies [e.g., *Gosling et*

al., 1995; *Kahler et al.*, 1996] showed that the shorter counterstreaming events tended to be grouped in time, suggesting that they may not be independent but rather part of the outflow from a single CME. As will be shown, this paper is consistent with that view.

The second widely used signature of interplanetary ejecta from CMEs, a magnetic cloud, was first identified by *Burlaga et al.* [1981] and *Klein and Burlaga* [1982] as large-scale rotations in the magnetic field accompanied by low ion temperatures and strong magnetic fields. Since all three criteria must be met to qualify as a cloud, clouds form a subset of well-defined ejecta encountered by spacecraft [*Gosling*, 1990; *Burlaga*, 1991]. The magnetic field data from clouds usually provide good fits to flux rope models and thus are usually assumed to take that form [e.g., *Burlaga*, 1988; *Lepping et al.*, 1990]. On a global scale the flux ropes are assumed to form loops with ends extending back toward the Sun. If both ends are fully connected to the Sun, the field lines in the rope are closed, implying coincidence between magnetic clouds and counterstreaming electrons. This paper determines the degree to which coincidence occurs within the boundaries of clouds identified in Wind data.

A few earlier studies addressing the relationship between magnetic clouds and counterstreaming electrons provide background for the present study. For the ISEE 3 data set covering the period August 1978 through October 1982, *Gosling* [1990] pointed out that 14 of the 15 clouds identified by *Zhang and Burlaga* [1988] contained counterstreaming intervals. In a case study of another cloud detected by ISEE 3, *Crooker et al.* [1990] showed that the cloud contained two intervals of counterstreaming and that these intervals together covered less than 50% of the structure. Subsequent studies of two clouds encountered by the Wind spacecraft showed even smaller percentages of counterstreaming [*Larson et al.*, 1997;

¹Center for Space Physics, Boston University, Boston, Massachusetts.

²Air Force Research Laboratory, Space Vehicles Directorate, Hanscom Air Force Base, Massachusetts.

³Laboratory for Extraterrestrial Physics, NASA Goddard Space Flight Center, Greenbelt, Maryland.

⁴Space Sciences Laboratory, University of California, Berkeley.

⁵Los Alamos National Laboratory, Los Alamos, New Mexico.

Crooker et al., 1998a]. In contrast, for those clouds observed at ISEE 3 that occurred at sector boundaries (about half), *Crooker et al.* [1998b] found that the counterstreaming intervals tended to extend well beyond the cloud boundaries, exceeding cloud length by more than a factor of 2. Finally, case studies by *Gosling et al.* [1995] and *Bothmer et al.* [1996] using Ulysses data from 4.6 AU and 1.4 AU, respectively, showed intermittent counterstreaming within and, in the latter case, also beyond a magnetic cloud.

The results of the above studies suggest that the degree of coincidence of counterstreaming electrons and magnetic clouds is highly variable. The purpose of the present paper is to document that variability by analyzing the percentage of time counterstreaming occurred during passage of a large number of magnetic clouds.

2. Analysis

Lists of magnetic clouds from two periods were used for this study. The first period, from August 1978 to September 1982, spans the maximum of solar cycle 21. It coincides with the ISEE 3 mission, from which suprathermal electron data from the Los Alamos solar wind plasma experiment are available for identifying counterstreaming events [*Gosling et al.*, 1987a]. As mentioned in section 1, during this period, 15 magnetic clouds were identified by *Zhang and Burlaga* [1988]. For 8 of these, we use the boundary identifications later refined by *Lepping et al.* [1990]. Some of the clouds were identified in near-Earth IMP 8 data, while the counterstreaming events within them were identified in upstream-libration-point ISEE 3 data. The lag time of less than an hour between measurements taken at the two spacecraft was ignored for the purposes of this study, since cloud boundaries were identified only to the nearest hour.

The list of clouds from the second period, February 1995 through November 1998, spans the minimum between solar cycles 22 and 23. It coincides with the beginning of the Wind mission, when the first 34 clouds (web-accessible from NASA Goddard Space Flight Center at http://lepmfi.gsfc.nasa.gov/mfi/mag_cloud_pub1.html) were identified in data from the Magnetic Field Investigation (MFI, R. P. Lepping, principal investigator) (cf. R. P. Lepping et al., Profile of a generic magnetic cloud at 1 AU for the quiet solar phase: Wind observations, submitted to *Journal of Geophysical Research*, 2000) (hereinafter referred to as Lepping et al., submitted manuscript, 2000). Corresponding suprathermal electron data from both the Three-Dimensional Plasma instrument (3DP, R. P. Lin, principal investigator) (web-accessible from Space Sciences Laboratory, University of California, Berkeley, at http://plasma2.ssl.berkeley.edu/wind3dp/sumplots/plot_search.html) and the Solar Wind Experiment (SWE, K. W. Ogilvie, principal investigator) were used to identify and confirm counterstreaming events.

To calculate the percentages of counterstreaming electrons coincident with the clouds, pitch angle spectrograms in the heat flux energy range, ~ 100 -200 eV, were scanned by eye, and boundaries of counterstreaming events were determined to the nearest 15 min. For cases with data gaps, if counterstreaming occurred at both ends of the gap, it was assumed to occur throughout the gap. On the other hand, if counterstreaming occurred at only one end, no assumption was made, and the gap was eliminated from the percentage calculation. For

the Wind data all gaps longer than 45 min were eliminated from the percentage calculation.

The process of selecting counterstreaming intervals is somewhat subjective. Although signatures tend to be uniform within candidate intervals, so that their boundaries are clear, whether to categorize a given interval as counterstreaming or not becomes questionable for pitch angle distributions approaching isotropy and for cases where flux in one of the counterstreaming directions is weak. Concerning the latter, *Pilipp et al.* [1987] note that highly unbalanced heat flux most likely indicates encounter with one leg of a closed structure that extends out into the heliosphere well beyond the spacecraft location [cf. *Kahler et al.*, 1999a]. Thus placing a limit on how weak the flux in one direction can be before an event is no longer classified as a bidirectional electron (BDE) event may, in effect, be placing a limit on how far a closed structure can extend from the Sun before it is considered open. In view of the expectation that counterstreaming and clouds should coincide, our calculated percentages include both unbalanced cases and cases approaching isotropy and thus represent the maximum possible closed flux. To give some measure of the resulting uncertainty, minimum as well as maximum percentages were calculated for the ISEE 3/IMP 8 cases. The minima were calculated using the list of counterstreaming intervals given by *Gosling et al.* [1987a] and unpublished lists assembled earlier for other studies [e.g., *Gosling et al.*, 1990]. These lists are conservative because they tend to exclude unbalanced or nearly isotropic cases. As a result, for some clouds there is a large difference between minimum and maximum percentages.

For completeness, heat flux dropout intervals, presumably representing fields disconnected from the Sun at both ends, were identified in the Wind data, following the method of *Larson et al.* [1997; see also *McComas et al.*, 1989; *Lin and Kahler*, 1992; *Larson et al.*, 2000]. Only cases with clear signatures covering a wide energy range were included in this category. Many of these contained residual counterstreaming, in contrast, for example, to the case analyzed by *Feldman et al.* [1999]. Thus uncertainty in heat flux dropout identification also maximizes our counterstreaming percentages. This effect is minimal, however, since most clouds show no evidence of dropouts.

As an example of our analysis procedure, heat flux data from SWE for the cloud on September 18-20, 1997, are shown in the top panel of Plate 1, with magnetic field latitude (θ) and longitude (ϕ) angles plotted in the panels below. The field rotation in the cloud is apparent in the field plots, where vertical lines mark the cloud boundaries. The colored bar below the heat flux data, labeled "BDE interval," where "BDE" stands for "bidirectional electrons" [*Gosling et al.*, 1987a], is orange where counterstreaming occurred. The heat flux spectrogram indicates counterstreaming where flux maxima lie near pitch angles of both 0° and 180° , corresponding to directions parallel and antiparallel to the magnetic field. The spectrogram shows that some counterstreaming precedes the cloud, as well, but this interesting point is not our focus here. The yellow intervals in the BDE bar indicate periods when Wind is magnetically connected to Earth's bow shock. In these intervals, counterstreaming may be a signature of bow shock acceleration rather than, or as well as, closed topology. The orange bar, including the yellow periods, represents most of the counterstreaming for

Table 1. Percent Counterstreaming (%BDE) in Clouds

Number	Cloud Start			Duration, hours	%BDE Min/Max	Diameter, AU
	Year	Date	Hour			
ISEE3/IMP8						
	1978	Aug. 27	1900	21	30/64	0.201
	1978	Sept. 29	1000	17	67	
	1978	Oct. 29	2300	25	39	0.219
	1979	April 3	2200	22	100	
	1979	Dec. 3	1100	29	24	
	1980	Feb. 16	0100	29	87	0.291
	1980	March 19	1800	41	68/84	0.297
	1980	Dec. 11	2300	32	100	
	1980	Dec. 19	1200	26	75/85	0.266
	1981	Feb. 7	0700	29	100	0.517
	1981	March 5	1300	18	94	0.262
	1981	Sept. 19	0700	13	0/37	
	1982	Feb. 12	0300	42	100	
	1982	Sept. 25	1700	22	0/75	
Wind						
1	1995	Feb 8	0300	20	65	0.224
2	1995	March 4	1100	18	77	0.192
3	1995	April 6	0700	12	29	0.103
4	1995	May 13	1000	7	17	0.173
5	1995	Aug. 22	2200	22	92	0.233
6	1995	Oct. 18	1900	30	48	0.263
7	1995	Dec. 16	0500	18	50	0.319
8	1996	May 27	1500	41	78	0.389
9	1996	July 1	1700	17	0	0.166
10	1996	Aug. 7	1300	22	5	0.216
11	1996	Dec. 24	0300	32	23	0.295
12	1997	Jan. 10	0500	22	27	0.205
13	1997	Feb. 10	0300	16	83	
14	1997	April 21	1500	41	83	0.399
15	1997	May 15	0900	17	2	0.185
16	1997	June 9	0200	22	6	0.289
17	1997	July 15	0600	20	30	0.149
18	1997	Aug. 3	1400	12	50	0.146
19	1997	Sept. 18	0000	61	83	0.337
20	1997	Sept. 21	2200	26	30	0.319
21	1997	Oct. 1	1600	32	100	0.501
22	1997	Oct. 10	2300	26	100	0.227
23	1997	Nov. 7	0500	32	70	0.316
24	1997	Nov. 22	1400	29	67	0.278
25	1998	Jan. 7	0300	32	79	0.252

Table 1. (continued)

Number	Cloud Start			Duration, hours	%BDE Min/Max	Diameter, AU
	Year	Date	Hour			
Wind (continued)						
26	1998	Jan. 8	1400	9	5	0.086
27	1998	Feb. 4	0400	43	68	0.296
28	1998	March 4	1400	41	15	0.384
29	1998	May 2	1200	30	90	0.531
30	1998	June 2	1000	6	0	0.073
31	1998	June 24	1400	27	76	0.289
32	1998	Aug. 20	1000	34	43	0.223
33	1998	Sept. 25	0500	33	100	0.538
34	1998	Nov. 8	1900	31	93	0.248

this case. Five brief, questionable intervals, ranging from 15 min to 3 hours 15 min, were also included in the percentage calculation. Most of these are not apparent in Plate 1 but are visible in the 3DP data (not shown).

All 48 clouds were analyzed in a similar manner, and the results are listed in Table 1 and displayed in Figures 1-4. For each cloud, Table 1 gives the start time, duration, and percent of its duration coincident with counterstreaming electrons. For cases with data gaps longer than 45 min the percentages are based on the cloud durations reduced by the gap lengths. Five of the 14 ISEE 3/IMP 8 clouds had intervals of unbalanced and/or nearly isotropic heat fluxes, as discussed above. (One of the 15 ISEE 3/IMP 8 clouds, in September 1979, was not included in the study because it contained saturated electron data in which counterstreaming boundaries could not be identified.) For these five both maximum and minimum percentages are listed. They differ the most for the September 25, 1982, cloud, where all counterstreaming was unbalanced and overall fluxes were weak.

Figure 1 is a histogram of the counterstreaming percentages in Table 1, where the maximum values for the ISEE 3/IMP 8 clouds were used. Shading differentiates clouds from the two different periods (and instruments). It shows that even

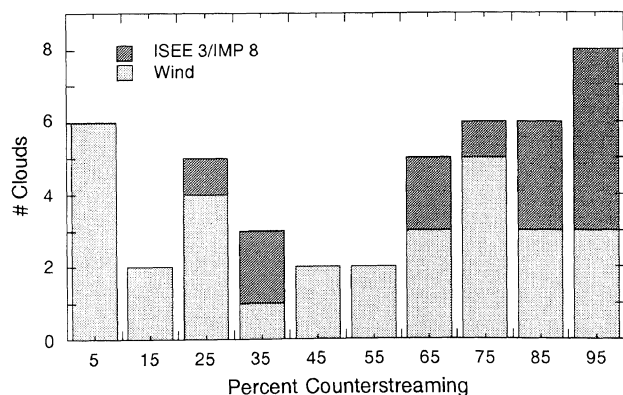


Figure 1. Distribution of the percentage of time during magnetic cloud passage when counterstreaming electrons were observed. Of the total of 48 clouds, the 14 detected by ISEE 3/IMP 8 occurred near solar maximum, while the 34 detected by Wind occurred near solar minimum.

when all possible counterstreaming is taken into account, clouds vary widely in the degree to which they are magnetically closed. For the Wind cases the distribution is nearly flat, implying that at least during solar minimum, clouds at 1 AU vary uniformly from being fully open to fully closed. In contrast, the ISEE 3/IMP 8 cases, although fewer in number, are distributed more heavily toward the closed end of the scale. Of the 14 cases, 11 have counterstreaming percentages greater than 60%. If we consider the minimum percentages instead, which are conservative for the ISEE 3/IMP 8 data, as discussed above, the net change in the distribution would be to move two cases from the 80-90% bin to the 0-10% bin. This would still leave a distribution weighted toward the closed end of the scale. Thus it seems unlikely that the apparent difference in the two distributions was caused by using data from different instruments, since data from the Wind instruments were processed to maximize detection of counterstreaming. Although more observations are needed at solar maximum to obtain statistically significant results, the apparent difference between the ISEE 3/IMP 8 and Wind distributions suggest that the time required for a magnetic cloud to become magnetically open is shorter at solar minimum compared to maximum.

Information about the durations of the counterstreaming intervals and how the intervals are distributed in the clouds is given in Figures 2 and 3 for the Wind data. Figure 2 shows the distribution of durations. The median value is 2.5 hours, the mean is 6.1 hours, and the maximum is 41.7 hours. Figure 3 was constructed to test for any pattern in the distribution of counterstreaming intervals within clouds. For example, if clouds become open through reconnection at their perimeters, then counterstreaming would tend to be missing near the cloud boundaries. The dark bars in Figure 3 represent counterstreaming intervals within each cloud, with one line per cloud, stacked from bottom to top in chronological order. Figure 3 shows essentially no pattern. Counterstreaming intervals appear to be distributed randomly throughout clouds.

Figure 3 also illustrates that heat flux dropouts, implying detached fields, are not major constituents of magnetic clouds. The exception is cloud 12, the January 10, 1997, case analyzed in detail by *Larson et al.* [2000]. Heat fluxes for the marked counterstreaming intervals were low, making these occurrences marginal between the counterstreaming and dropout categories.

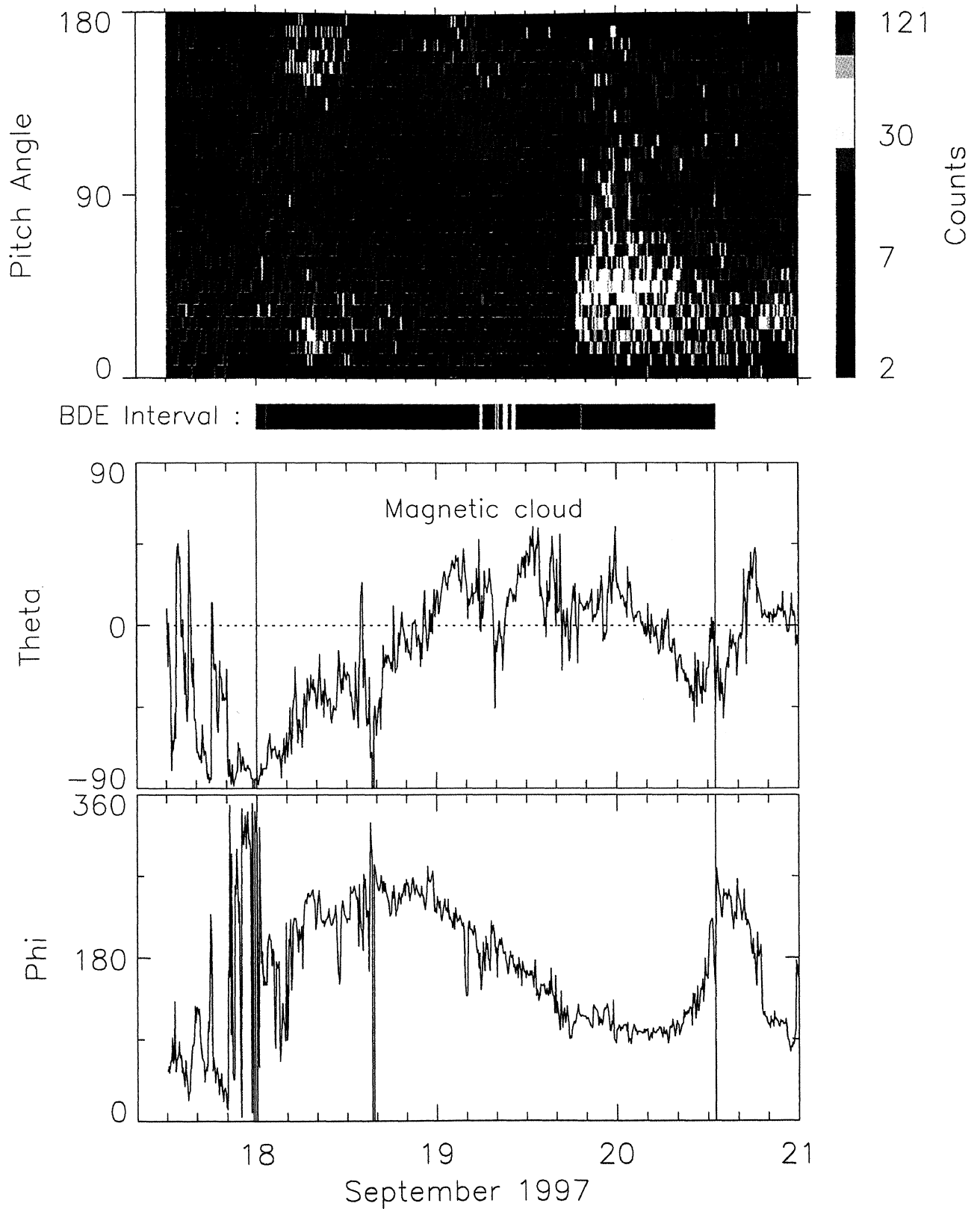


Plate 1. Pitch angle spectrogram of 91-97 eV electrons and time variations of magnetic field latitude θ and longitude ϕ during passage of a magnetic cloud. Vertical lines mark the cloud boundaries. The colored bar below the spectrogram indicates intervals of counterstreaming (orange), bow shock connection (yellow), and questionable or no counterstreaming (green).

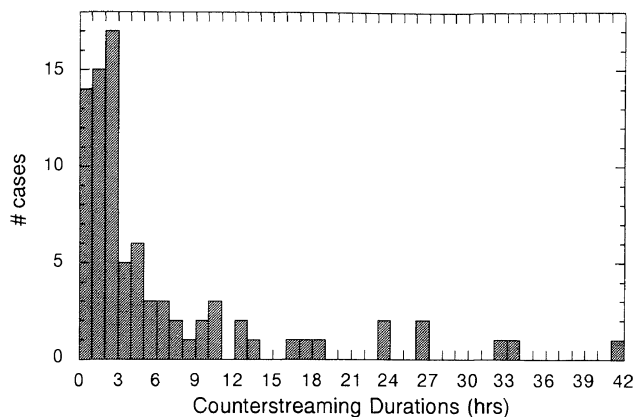


Figure 2. Distribution of the durations of counterstreaming electron intervals within the 34 clouds observed by Wind.

One clear pattern that does arise from this analysis is shown in Figure 4. There is a linear correlation between the percentage of counterstreaming and the size of the cloud. This result first became apparent in a plot of percent counterstreaming against cloud duration, from Table 1. The correlation coefficient between these values is 0.44. The correlation increased to 0.58, however, when the cloud durations were replaced by the cloud diameters in Table 1, as plotted in Figure 4. The diameters were obtained from model fits to force-free flux ropes [Lepping *et al.*, 1990, submitted manuscript, 2000].

The relationship in Figure 4 was checked for the possibility that it might only be a reflection of a bogus anticorrelation between cloud diameter and angle between the cloud axis and the Sun-Earth line (cone angle). This kind of anticorrelation can result from the modeling procedure coupled with a possible higher probability of misidentification of open for closed fields in the legs of ropes, where the cone angle is small and counterstreaming is unbalanced. Accordingly, cloud diameter was plotted against cone angle, but no relationship was found. Modeling also offered the opportunity to check whether the percent of counterstreaming in a cloud depends upon depth of penetration. This would be the case, for example, if closed fields tended to be concentrated near the core. Percent counterstreaming was thus plotted against impact parameter, that is, the percent of the radius spanning the minimum distance between the cloud axis and the spacecraft, but, again, no relationship was found.

3. Discussion

Since magnetic clouds are selected on the basis of multiple criteria and provide good fits to flux rope models, it seems appropriate to treat them as coherent entities. The question then arises as to why counterstreaming suprathermal electrons in clouds usually do not show the same coherence but, rather, occur intermittently throughout clouds. One possible answer is that clouds are composite structures, possibly consisting of multiple flux ropes [e.g., Osherovich *et al.*, 1999; Kahler *et al.*, 1999b; Vandas *et al.*, 1999]. Another possible answer draws on the modeling of Gosling *et al.* [1995], who demonstrated that the nested coiled field lines forming a

coherent flux rope can independently be open, closed, or disconnected owing to remote reconnection which eventually releases the rope. A variation of this pattern has been suggested by Larson *et al.* [1997] and Crooker *et al.* [1998a], who analyzed magnetic clouds that were primarily open, with one leg connected to an active region which periodically emitted energetic electrons [cf. Mazur *et al.*, 1998]. In these cases, the data were consistent with remote reconnection in that leg of the flux rope loop. Thus, in either variation, remote reconnection may be responsible for opening what originally were entirely closed magnetic fields in magnetic clouds.

In principle, one might expect to gain information on the rate of remote reconnection from the correlation between the percentage of counterstreaming and cloud size. If we make the simplifying assumption that the reconnection electric field

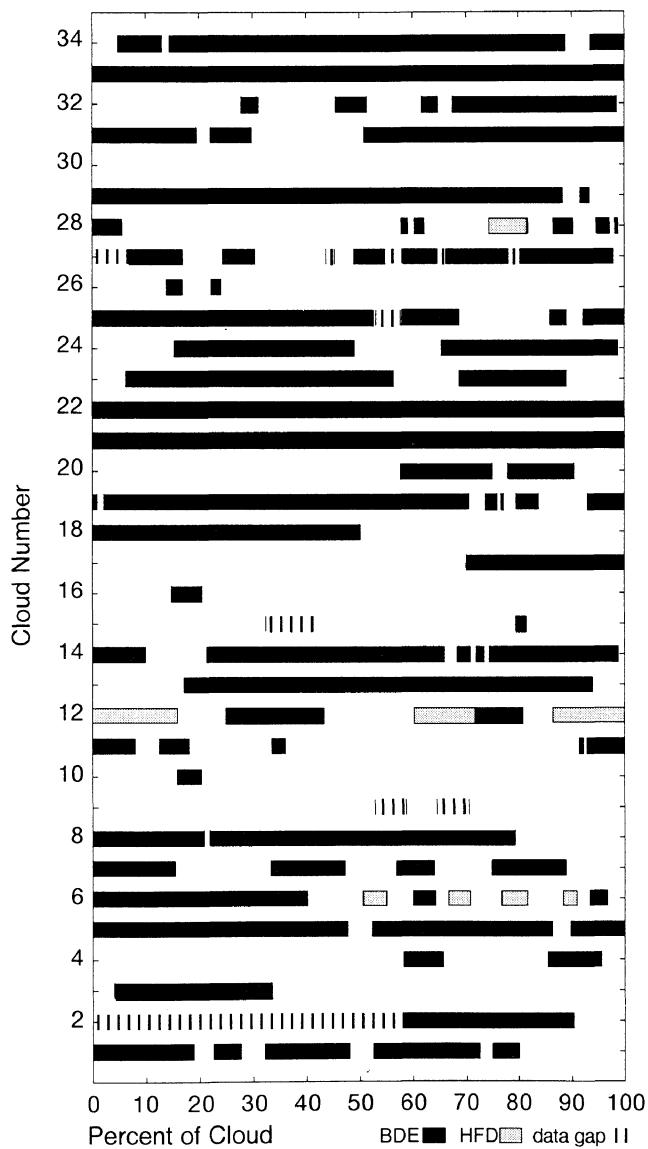


Figure 3. Stacked bar charts, one for each of 34 clouds observed by Wind, illustrating the distribution of counterstreaming (BDE) and heat flux dropout (HFD) intervals within the clouds.

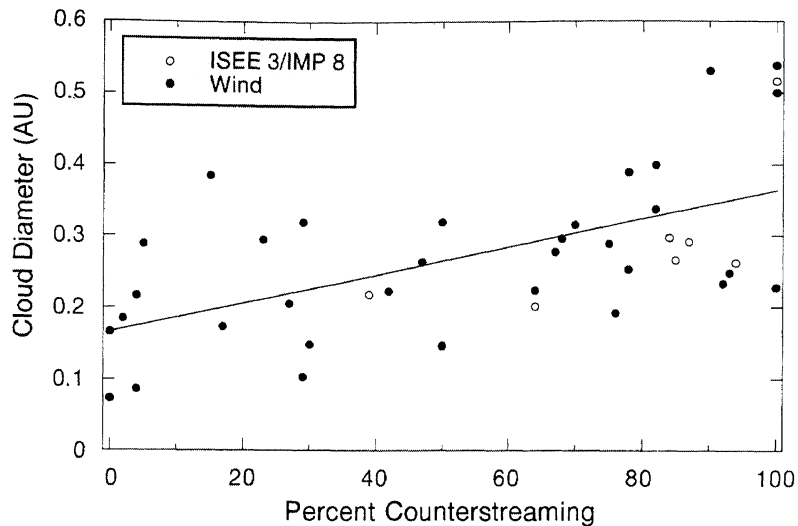


Figure 4. Scatterplot of percentage of counterstreaming electrons in a cloud against modeled cloud diameter for 7 clouds detected by ISEE 3/IMP 8 [Lepping *et al.*, 1990] and 33 clouds detected by Wind.

E_m is constant, in which case the reconnection rate depends upon the length over which it extends, and if that length, for example, is the circumference of the flux rope, proportional to radius R , then those clouds with the largest areas, proportional to R^2 , would have the highest percentage of remaining closed flux by the time the cloud reaches 1 AU. The relationship between the percentage of counterstreaming and cloud radius would be just a reflection of the ratio of area to perimeter, from which one could then derive a value for E_m . In practice, this idea fails because it predicts a nonlinear relationship between the percentage of counterstreaming %BDE and R of the following form: %BDE = $100 - E_m K/R$, where K is a factor containing the travel time from Sun to Earth and the strength of the magnetic field at the merging site and is assumed constant here. Although %BDE increases with increasing R , the relationship yields a family of curves which rise so steeply at large values that none can provide a reasonable fit to the points in Figure 4. This relationship applies not only to the case of reconnection at the outer boundary of the rope but also to reconnection at the boundary of an internally growing bundle of open flux, a more realistic geometry in view of the random occurrence of counterstreaming within clouds shown in Figure 3. Nevertheless, this analysis indicates that these simple geometries and constant reconnection electric fields do not apply to magnetic clouds assimilating into the solar wind.

There is one aspect of this study which does not appear to fit the view that clouds are in the process of becoming magnetically open as they pass over a spacecraft. If this were the case, one would expect the rate of occurrence of counterstreaming to decrease from the beginning to the end of cloud passage. Figure 3 shows that while some clouds follow this pattern, especially those near the bottom of the figure, others do not, and some even display an inverse of the pattern. A view more consistent with Figure 3 is that the process of becoming magnetically open does not occur gradually but rather in sporadic episodes, where large bundles of field lines reconnect over a short period of time.

The solar cycle variation of the percentage of closed flux in clouds suggested by Figure 1, with more closed flux at solar

maximum, may just be a reflection of the correlation with cloud size, with larger clouds at solar maximum. The number of cases analyzed, however, is too small to be conclusive on this point. From the values in Figure 4, the average diameter for the ISEE 3/IMP 8 cases is 0.29 AU, insignificantly different from the average of 0.27 AU for the Wind cases, in view of the amount of scatter in the figure.

We note that the extension of counterstreaming beyond cloud boundaries and the relationship of this pattern to sector boundaries found in the ISEE 3 data by Crooker *et al.* [1998b] were not analyzed in the Wind data for this study, primarily because the magnetic signatures of the sector structure in the Wind data tended to be complex owing to the low inclination of the heliospheric current sheet [e.g., Szabo *et al.*, 1999; Crooker, 1999]. Nevertheless, these issues are part of the larger problem of understanding the magnetic topology of magnetic clouds in the context of heliospheric structure and are mentioned here for completeness.

4. Conclusions

Although magnetic clouds at 1 AU are observed as coherent structures, most often they comprise a random mix of several intertwined volumes of magnetically open and closed field lines. The largest clouds have the most closed flux, and clouds at solar maximum appear to have more closed flux than those at solar minimum. The reconnection responsible for converting closed to open flux in a magnetic cloud most likely proceeds remotely and sporadically until the field lines which originally connected the cloud to the Sun become part of the ambient solar wind outflow.

Acknowledgments. We thank David Sibeck for help in identifying counterstreaming signatures created by backstreaming electrons accelerated at Earth's bow shock. This research was supported by the National Science Foundation under grant ATM98-050604 and by the National Aeronautics and Space Administration under grant NAG5-7049. Work at Los Alamos was performed under the auspices of the U.S. Department of Energy, also with support from NASA.

Janet G. Luhmann thanks Joseph A. Mazur and Tamitha L. Mulligan for their assistance in evaluating this paper.

References

- Bothmer, V., et al., Ulysses observations of open and closed magnetic field lines within a coronal mass ejection, *Astron. Astrophys.*, 316, 493-498, 1996.
- Burlaga, L. F., Magnetic clouds and force-free fields with constant alpha, *J. Geophys. Res.*, 93, 7217-7224, 1988.
- Burlaga, L. F., Magnetic clouds, in *Physics of the Inner Heliosphere II*, edited by R. Schwenn and E. Marsch, pp. 1-22, Springer-Verlag, New York, 1991.
- Burlaga, L., E. Sittler, F. Mariani, and R. Schwenn, Magnetic loop behind an interplanetary shock: Voyager, Helios, and IMP 8 observations, *J. Geophys. Res.*, 86, 6673-6684, 1981.
- Crooker, N. U., Heliospheric current sheet structure, in *Solar Wind Nine*, edited by S. Habbal et al., pp. 93-98, Am. Inst. of Phys., New York, 1999.
- Crooker, N. U., J. T. Gosling, E. J. Smith, and C. T. Russell, A bubblelike coronal mass ejection flux rope in the solar wind, in *Physics of Magnetic Flux Ropes*, *Geophys. Monogr. Ser.*, vol. 58, edited by C. T. Russell, E. R. Priest, and L. C. Lee, pp. 365-371, AGU, Washington, D. C., 1990.
- Crooker, N. U., et al., Sector boundary transformation by an open magnetic cloud, *J. Geophys. Res.*, 103, 26,859-26,868, 1998a.
- Crooker, N. U., J. T. Gosling, and S. W. Kahler, Magnetic clouds at sector boundaries, *J. Geophys. Res.*, 103, 301-306, 1998b.
- Feldman, W. C., R. M. Skoug, J. T. Gosling, D. J. McComas, R. L. Tokar, L. F. Burlaga, N. F. Ness, and C. W. Smith, Shapes of solar wind suprathermal electron velocity distributions during the 4-5 February, 1998, interplanetary coronal mass ejection, *Geophys. Res. Lett.*, 26, 2613-2616, 1999.
- Gosling, J. T., Coronal mass ejections and magnetic flux ropes in interplanetary space, in *Physics of Magnetic Flux Ropes*, *Geophys. Monogr. Ser.*, vol. 58, edited by C. T. Russell, E. R. Priest, and L. C. Lee, pp. 343-364, AGU, Washington, D. C., 1990.
- Gosling, J. T., D. N. Baker, S. J. Bame, W. C. Feldman, and R. D. Zwickl, Bidirectional solar wind electron heat flux events, *J. Geophys. Res.*, 92, 8519-8535, 1987a.
- Gosling, J. T., M. F. Thomsen, S. J. Bame, and R. D. Zwickl, The eastward deflection of fast coronal mass ejecta in interplanetary space, *J. Geophys. Res.*, 92, 12,399-12,406, 1987b.
- Gosling, J. T., S. J. Bame, D. J. McComas, and J. L. Phillips, Coronal mass ejections and large geomagnetic storms, *Geophys. Res. Lett.*, 17, 901-904, 1990.
- Gosling, J. T., D. J. McComas, J. L. Phillips, and S. J. Bame, Geomagnetic activity associated with earth passage of interplanetary shock disturbances and coronal mass ejections, *J. Geophys. Res.*, 96, 7831-7839, 1991.
- Gosling, J. T., J. Birn, and M. Hesse, Three-dimensional magnetic reconnection and the magnetic topology of coronal mass ejection events, *Geophys. Res. Lett.*, 22, 869-872, 1995.
- Kahler, S. W., N. U. Crooker, and J. T. Gosling, The topology of intrasector reversals of the interplanetary magnetic field, *J. Geophys. Res.*, 101, 24,373-24,382, 1996.
- Kahler, S. W., N. U. Crooker, and J. T. Gosling, The polarities and locations of interplanetary coronal mass ejections in large interplanetary magnetic sectors, *J. Geophys. Res.*, 104, 9919-9924, 1999a.
- Kahler, S. W., N. U. Crooker, and J. T. Gosling, A magnetic polarity and chirality analysis of ISEE 3 interplanetary magnetic clouds, *J. Geophys. Res.*, 104, 9911-9918, 1999b.
- Klein, L. W., and L. F. Burlaga, Interplanetary magnetic clouds at 1 AU, *J. Geophys. Res.*, 87, 613-624, 1982.
- Larson, D. E., et al., Tracing the topology of the October 18-20, 1995 magnetic cloud with $\sim 0.1 - 10^2$ keV electrons, *Geophys. Res. Lett.*, 24, 1911-1914, 1997.
- Larson, D. E., R. P. Lin, and J. Steinberg, Extremely cold electrons in the January 1997 magnetic cloud, *Geophys. Res. Lett.*, 27, 157-160, 2000.
- Lepping, R. P., J. A. Jones, and L. F. Burlaga, Magnetic field structure of interplanetary magnetic clouds at 1 AU, *J. Geophys. Res.*, 95, 11,957-11,965, 1990.
- Lin, R. P., and S. W. Kahler, Interplanetary magnetic field connection to the sun during electron heat flux dropouts in the solar wind, *J. Geophys. Res.*, 97, 8203-8209, 1992.
- Mazur, J. E., G. M. Mason, J. R. Dwyer, and T. T. von Rosenvinge, Solar energetic particles inside magnetic clouds observed with the Wind spacecraft, *Geophys. Res. Lett.*, 25, 2521-2524, 1998.
- McComas, D. J., J. T. Gosling, J. L. Phillips, S. J. Bame, J. G. Luhmann, and E. J. Smith, Electron heat flux dropouts in the solar wind: Evidence for interplanetary magnetic field reconnection?, *J. Geophys. Res.*, 94, 6907-6916, 1989.
- Montgomery, M. D., J. R. Asbridge, S. J. Bame, and W. C. Feldman, Solar wind electron temperature depressions following some interplanetary shock waves: Evidence for magnetic merging?, *J. Geophys. Res.*, 79, 3103-3110, 1974.
- Neugebauer, M., and R. Goldstein, Particle and field signatures of coronal mass ejections in the solar wind, in *Coronal Mass Ejections*, *Geophys. Monogr. Ser.*, vol. 99, edited by N. U. Crooker, J. A. Joselyn, and J. Feynman, pp. 245-251, AGU, Washington, D. C., 1997.
- Osherovich, V. A., J. Fainberg, and R. G. Stone, Multi-tube model for interplanetary magnetic clouds, *Geophys. Res. Lett.*, 26, 401-404, 1999.
- Pilipp, W. G., H. Miggenrieder, K.-H. Mylhuser, H. Rosenbauer, R. Schwenn, and F. M. Neubauer, Variations of electron distribution functions in the solar wind, *J. Geophys. Res.*, 92, 1103-1118, 1987.
- Szabo, A., D. E. Larson, and R. P. Lepping, Heliospheric current sheet on small scale, in *Solar Wind Nine*, edited by S. Habbal et al., pp. 589-592, Am. Inst. of Phys., New York, 1999.
- Vandas, M., S. Fischer, and A. Geranos, Double flux rope structure of magnetic clouds?, in *Solar Wind Nine*, edited by S. Habbal et al., pp. 127-130, Am. Inst. of Phys., New York, 1999.
- Zhang, G., and L. F. Burlaga, Magnetic clouds, geomagnetic disturbances, and cosmic ray decreases, *J. Geophys. Res.*, 93, 2511-2518, 1988.
- Zwickl, R. D., J. R. Asbridge, S. J. Bame, W. C. Feldman, J. T. Gosling, and E. J. Smith, Plasma properties of driver gas following interplanetary shocks observed by ISEE 3, in *Solar Wind Five*, edited by M. Neugebauer, *NASA Conf. Publ. CP-2280*, 711-717, 1983.

N. U. Crooker, S. Shodhan, and G. L. Siscoe, Center for Space Physics, Boston University, 725 Commonwealth Avenue, Boston, MA 02215. (crooker@bu.edu; shodhan@bu.edu; siscoe@bu.edu)

R. J. Fitzenreiter and R. P. Lepping, Laboratory for Extraterrestrial Physics, NASA Goddard Space Flight Center, Greenbelt, MD 20771. (u3rjf@leprjf.gsfc.nasa.gov; rpl@leprpl.gsfc.nasa.gov)

J. T. Gosling, Los Alamos National Laboratory, Group NIS-1, MS D466, Los Alamos, NM 87545. (jgosling@lanl.gov)

S. W. Kahler, Air Force Research Laboratory, Space Vehicles Directorate, 29 Randolph Road, Hanscom AFB, MA 07131-3010. (kahler@plh.af.mil)

D. E. Larson, Space Sciences Laboratory, University of California, Berkeley, CA 94720-7450. (davin@ssl.berkeley.edu)

(Received February 24, 2000; revised May 19, 2000; accepted May 19, 2000.)